DOI: 10.1021/cg901153q

CRYSTAL GROWTH & DESIGN Article

2010, Vol. 10 754–760

Conformational Polymorphism of a Simple Tripodal Podand Bearing Nitro Functionality

Sandeep Kumar Dey and Gopal Das*

Department of Chemistry, Indian Institute of Technology Guwahati, Assam-781039, India

Received September 21, 2009; Revised Manuscript Received November 12, 2009

ABSTRACT: Tris[4-(nitrophenyloxy)ethyl]amine (**L**), a simple tripodal podand, may be reproducibly crystallized in either of three polymorphic forms. An understanding of the structural features associated with polymorphism in **L** has been made in terms of morphology, single-crystal structure, powder X-ray diffraction, and differential scanning calorimetric measurements. Polymorphs I, II, and III crystallize in three different crystal systems—triclinic ($P\bar{1}$), monoclinic ($P2_1/n$), and orthorhombic ($Pna2(1)$), respectively—and single-crystal X-ray analysis revealed conformational differences in the arrangement of the flexible arms when crystallized from solutions under different growth conditions. The conformational difference results principally from the bridge-head amino torsion τ_{amino} ($C-N1_{amino}-C-C$) relative to the *p*-nitrophenol fragment. The different polymorphs display a range of different 3D hydrogen bonding arrangements, constructed from an intermolecular $C-H\cdots O$ hydrogen bonding array. The supramolecular self-assembly features in the three forms are guided by the control methylene $C-H\cdots N_{amino}$ dimeric interaction in form I, the $\pi\cdots\pi$ interaction in form II, and a weak $C-H\cdots\pi$ interaction in form III that differentiate the overall packing in the three forms.

1. Introduction

Polymorphism, as defined in McCrone's words, is "the ability of a given element or compound to crystallize as more than one distinct crystal species".[1] Some crystals are conformational polymorphs because of conformational variations of molecules in the solid state.[2] Because of the dissimilarity in solid-state structures, polymorphs of the substance can vary significantly in their physicochemical properties. Polymorphism has emerged as a solid-state property of outstanding fundamental and practical importance; the impact is evident by an outburst of publications, patents, conferences, and special issues of journals on this enigmatic phenomenon.[3] One of the main objectives in the study of polymorphism is to understand the effect of various parameters of a crystallization experiment in controlling the nucleation to obtain a desired polymorph.[4] The effect of solvent of crystallization, an important parameter influencing nucleation, continues to be the subject of investigations.[5] However, the control of crystal and network structures in a predictable manner still remains an elusive task because of the delicate balance and competition between directional noncovalent interactions, such as hydrogen bonds, and nondirectional noncovalent interactions, such as van der Waals (dispersive) packing forces. Since the physicochemical properties of a compound can differ critically from one form to another, inducing and controlling a specific polymorph is of utmost importance, particularly in the context of syntheses of drugs and pharmaceuticals.[6] The design and synthesis of new materials with desired chemical and physical properties have been of recent interest, and this involves the generation and study of structural motifs in crystals, which are essentially guided by precise topological control through the manipulation of weak intermolecular interactions. There are a rich variety of intermolecular interactions that serve as tools in engineering such molecular assemblies.[7] Polymorphism perhaps tends to be prominent in molecules that contain multiple hydrogen-bonding moieties, thereby forming multiple supramolecular synthons,[8] and/or conformational flexibility,[9] as exemplified in a number of active pharmaceutical ingredients (APIs).[10] Isotropic van der Waals interactions also play an important role in generating different molecular assemblies. Conformational polymorphism has attracted considerable attention due to the fact that it provides ideal systems for the study of structure–property relationships,[11] the effect of crystal forces on molecular conformation,[12] molecular-level control of crystallization,[13] and the prediction[14] and design[15] of crystal structures.

Ideally, one would like to obtain a particular polymorph with one set of experimental crystallization conditions and another polymorph with another set. However, this may not always be possible and polymorphs may be obtained concomitantly whatever be the experimental conditions employed. In such cases, rapid identification and separation of the polymorphs is necessary. The polymorph formation of a given substance lies in a compromise between inter- and intramolecular interactions which can be affected by crystallization conditions. The structures and properties of tripodal ligands have been well studied.[16] However, these compounds have not received any attention in the context of polymorphism regardless of their intrinsic conformational flexibility.[17] During our systematic investigation of tripodal receptors,[18] we have obtained three conformational polymorphs (I, II, and III) of a podand **L** (Scheme 1) from different crystallization conditions. Differences in molecular conformation of the polymorphs are very likely a result of torsion angle differences. Here, we report the solvent mediated reproducible crystallization of **L** into three different polymorphic forms, a discussion of their crystal structures, and the results of thermal studies along with their powder XRD and FT-IR patterns.

*E-mail: gdas@iitg.ernet.in.

 Published on Web 12/11/2009

2. Experimental Section

2.1. General. All reagents and solvents were obtained from commercial sources and used as received. Propanol was dried using anhydrous calcium chloride and distilled freshly following a standard procedure. The IR spectra were recorded on a Perkin-Elmer-Spectrum One FT-IR spectrometer with KBr disks in the range 4000−400 cm^{-1}. Powder X-ray diffraction data were recorded using a Seifert powder X-ray diffractometer (XRD 3003TT) with a Cu Kα source (λ = 1.54 Å) on a glass surface of an air-dried sample. The thermal analyses of the polymorphs were performed by using an SDTA 851 e TGA thermal analyzer (Mettler Toledo) with a heating rate of 2 °C per min in a N_2 atmosphere. Optical micrograph images were taken in a *Zeiss-Axio Cam-MRc* microscope fitted with a digital camera of air-dried samples on glass microslides.

2.2. Synthesis of L. Podand **L** has been prepared by modification of a known literature procedure.[19] To a solution of 4-nitrophenol (5 g, 36 mmol) in dry *n*-propanol (30 mL) was added crushed NaOH (1.77 g, 43 mmol), and the solution was stirred at room temperature for 1 h. To the resulting suspension, tris(2-chloroethyl)amine hydrochloride (2.88 g, 12 mmol) was added at once, and the mixture was stirred for another 1 h at room temperature. For completion of the reaction, the mixture was refluxed for 8 h followed by removal of the solvents under reduced pressure and addition of 20 mL of cold water. The expected product was extracted from this mixture, with 3 × 30 mL of $CHCl_3$. The organic layer was washed with water and dried over anhydrous Na_2SO_4, and solvents were removed under reduced pressure. The crude product was purified by column chromatography with 75% ethyl acetate (in petroleum ether) as the eluent. The desired compound was a pale yellow solid. Yield 65%.

2.3. X-ray Crystallography. In each case, a crystal of suitable size was selected from the mother liquor and immersed in silicone oil, and then it was mounted on the tip of a glass fiber and cemented using epoxy resin. The intensity data were collected using a Bruker SMART APEX-II CCD diffractometer, equipped with a fine focus 1.75 kW sealed tube Mo Kα radiation (λ = 0.71073 Å) at 298(3) K, with increasing ω (width of 0.3° per frame) at a scan speed of 3 s/frame. The SMART software was used for data acquisition. Data integration and reduction were undertaken with SAINT and XPREP[20] software. Multiscan empirical absorption corrections were applied to the data using the program SADABS.[21] Structures were solved by direct methods using SHELXS-97 and refined with full-matrix least-squares on F^2 using SHELXL-97.[22] All non-hydrogen atoms were refined anisotropically. Hydrogen atoms attached to all carbon atoms were geometrically fixed while the hydrogen atoms of the tertiary amino nitrogen of the salts were located from the difference Fourier map, and the positional and temperature factors are refined isotropically. Structural illustrations have been drawn with ORTEP-3 for Windows.[23]

Scheme 1. Molecular Structure of Tripodal Podand L

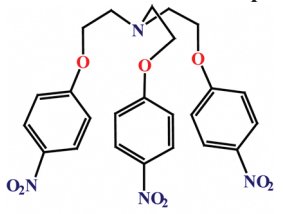

L

3. Results and Discussions

3.1. Crystal Structure Studies. The crystallographic data and details of data collection for polymorphs I, II, and III are given in Table 1. Solvent-induced conformational polymorphism of tripodal podand **L** arises from (i) the intrinsic conformational flexibility of the molecule, (ii) the correlation between the hydrogen bond donor ability of the alkyl groups and the hydrogen bond acceptor ability of the oxygen atoms of nitro groups, and (iii) the nature of crystallization solvents. Crystal structure analyses reveal the presence of interesting supramolecular features in all three polymorphs. There are no intramolecular noncovalent interactions between the tripodal arms in polymorphs I and III whereas polymorph II displays an intramolecular edge-to-face interaction between the phenyl rings of the two proximal arms. The presence of various types of intermolecular noncovalent interactions between the tripodal units results in markedly different crystal packing in the three forms. The nitro oxygen atoms act as acceptor and are involved in multiple C−H···O intermolecular hydrogen bonding in all three forms. Conformational polymorphism in podand **L** is also reflected from their different crystal morphologies.

3.1.1. Polymorph I. This form crystallizes in the triclinic space group $P\bar{1}$ with Z = 2. An ORTEP plot of polymorph I is shown in Figure 1a along with the atom numbering scheme. The torsion τ_{ether} involving $N1_{amino}$−C−C−O_{ether} is in the folded conformation for the two arms composed of the ethereal oxygens O1 and O4 and is in the extended conformation for the third arm composed of the ethereal

Table 1. Crystallographic Data for Polymorphs I, II, and III

	I	II	III
formula	$C_{24}H_{24}N_4O_9$	$C_{24}H_{24}N_4O_9$	$C_{24}H_{24}N_4O_9$
fw	512.47	512.47	512.47
crystal system	triclinic	monoclinic	orthorhombic
space group	$P\bar{1}$	$P21/n$	$Pna2(1)$
a (Å)	9.252(2)	10.5408(6)	23.1068(15)
b (Å)	11.950(3)	19.9111(12)	23.107
c (Å)	12.445(3)	11.8327(8)	4.6074(4)
α (deg)	73.244(14	90.00	90.00
β (deg)	78.589(14)	105.594(3)	90.00
γ (deg)	70.475(14)	90.00	90.00
V (Å)	1233.9(5)	2392.0(3)	2460.0(3)
Z	2	4	4
T (K)	298(2)	298(2)	298(2)
μ (cm^{-1})	0.107	0.109	0.108
d_{cal} (g cm^{-3})	1.379	1.429	1.386
cryst dimens (mm^3)	0.39 × 0.31 × 0.19	0.35 × 0.29 × 0.21	0.30 × 0.22 × 0.17
no. of reflns collected	5904	5786	5963
no. of unique reflns	2884	3323	4803
no. of params	334	334	335
R1; wR2 ($I > 2\sigma(I)$)	0.0459; 0.1318	0.0427; 0.1178	0.0522; 0.1348
R(int)	0.0326	0.0615	0.1149
GOF ($F2$)	1.016	0.954	0.921

oxygen O7 (Table 2). The two tripodal molecules of the unit cell are oriented in the opposite direction with a strong dimeric association *via* the C−H···N hydrogen bond involving the apical nitrogen N1 of either unit with the methylene hydrogen H10B of the adjacent unit, forming a six membered hydrogen bonded ring (N1···C10 = 3.704 Å, ∠C10−H10B···N1 = 175.40°), as depicted in Figure 1b. The dimers are further well organized *via* intermolecular C−H···O hydrogen bonding interactions between the alkyl hydrogens with one or both of the oxygen atoms from each nitro group generating a 3D sheetlike arrangement of tripodal dimers when viewed along the crystallographic *a* axis (Figure 1c). The nitro oxygens (O3, O5, O6, O8, and O9) act as acceptors in C−H···O intermolecular hydrogen bonding with C···O distances and C−H···O angles ranging from 3.135 to 3.557 Å and from 119.51 to 167.72°, respectively (Table 3). The nitro oxygen atoms O3, O5, O6, and O8 are hydrogen bonded to alkyl hydrogens H24, H17A, H4, and H8, respectively, whereas O9 forms bifurcated acceptor hydrogen bonds to aromatic protons H15 and H23 of a dimer (Table 3). Overall noncovalent interactions in the solid-state result in the formation of three different types of hydrogen bonded ring structures named as A, B, and C. The repeated formation of an AB diad ring and a CBC type triad is shown in Figure 1d.

3.1.2. Polymorph II. This form crystallizes in the monoclinic space group $P2_1/n$ with $Z = 4$. An ORTEP plot of polymorph II is shown in Figure 2a along with the atom numbering scheme. The torsion angles τ_{ether} ($N1_{amino}$−C−C−O_{ether}) are all in the folded conformation for the three tripodal arms, which is significantly different from the case for the other two forms (Table 2). There is an intramolecular edge-to-face (C−H···π) interaction between H20 and the phenyl ring involving carbon atoms C11−C16 (C2g) (C20···C2g = 4.018 Å, ∠C20−H20···C2g = 151.71°). The tripodal units are self-assembled *via* π···π stacking and intermolecular C−H···O hydrogen bonding interactions between the alkyl hydrogens with one or both the oxygens from two nitro groups involving nitrogen N3 and N4. In addition, there are intermolecular nitro−nitro electrostatic interactions involving all three nitro groups (N3···O5 = 3.018 Å and N4···O2 = 2.873 Å) and a weak intermolecular edge-to-face interaction between H15 and the phenyl ring involving carbon atoms C3−C8 (C1g) (C15···C1g = 4.198 Å, ∠C15−H15···C1g = 164.57°). The phenyl ring (C1g) attached to oxygen O1 of a tripodal unit is in π···π interaction with the phenyl ring (C3g) bonded to oxygen O7 of another tripodal moiety, creating a one-dimensional chain along the *c* axis (Figure 2b). The distance between the centroids of the π···π stacked phenyl rings (C1g and C3g) is 3.734 Å. The π···π interaction between two tripodal units is facilitated due to such an orientation of the tripodal receptor arms that two arms

Table 2. Molecular Conformation: Relevant Torsion Angles

	I	II	III
(a) Torsion Involving $N1_{amino}CCO_{ether}$ (τ_{ether})			
N1−C1−C2−O1	−75.86(2)	65.82(2)	−69.96(2)
N1−C9−C10−O4	79.04(2)	75.36(1)	65.77(3)
N1−C17−C18−O7	−168.72(1)	70.33(1)	−169.08(2)
(b) Torsion Involving $CCO_{ether}C_{phenyl}$ (τ_{phenyl})			
C1−C2−O1−C3	179.61(1)	−177.34(1)	−170.38(2)
C9−C10−O4−C11	−179.20(1)	−174.42(1)	178.89(2)
C17−C18−O7−C19	−173.33(1)	−168.25(1)	177.56(2)
(c) Torsion Involving $CN1_{amino}CC$ (τ_{amino})			
C1−N1−C9−C10	−56.66(2)	−142.52(1)	64.88(3)
C1−N1−C17−C18	159.22(1)	87.99(1)	79.45(2)
C9−N1−C1−C2	−57.88(2)	−71.56(2)	97.81(2)
C9−N1−C17−C18	−71.7(2)	−131.00(1)	−145.26(2)
C17−N1−C1−C2	69.58(2)	68.78(2)	−126.58(2)
C17−N1−C9−C10	175.70(1)	77.45(2)	−70.13(3)

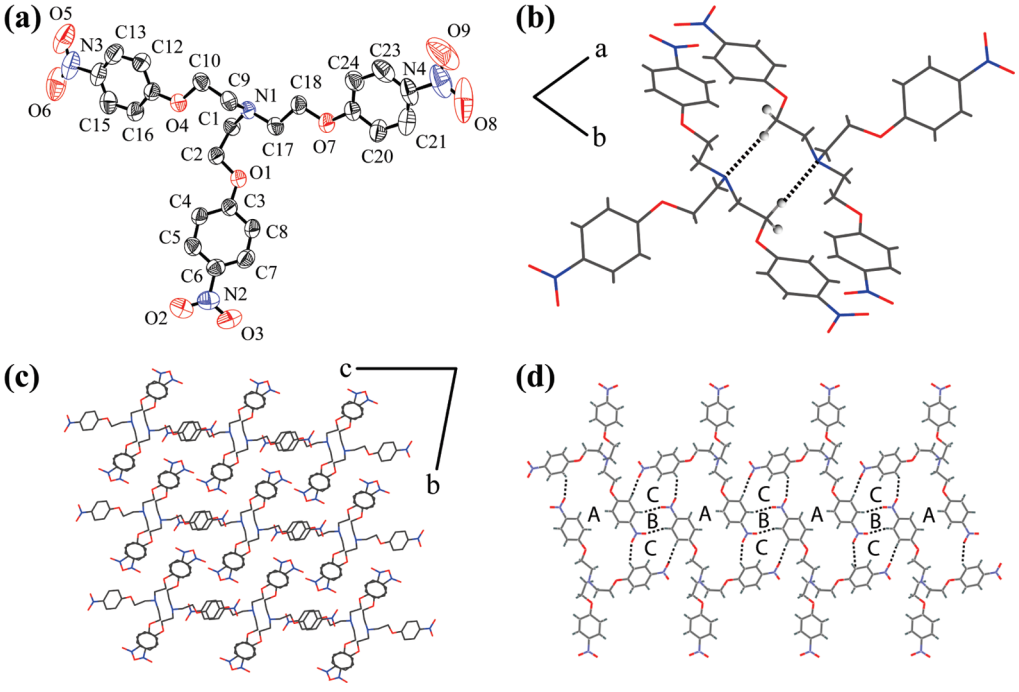

Figure 1. (a) ORTEP plot (50% probability ellipsoids) of polymorph I; (b) C−H···N dimeric interaction between two tripodal molecules in the unit cell; (c) crystal packing diagram of polymorph I viewed along the crystallographic *a* axis; (d) repeating formation of C−H···O hydrogen bonded rings AB diad and CBC triad.

involving oxygen atoms O1 and O7 of an unit are placed almost opposite and parallel to each other and probably due to the presence of intermolecular C−H···O interaction between nitro oxygen O8 and methylene hydrogen H9A. The $\pi\cdots\pi$ stacked one-dimensional chain is further cross-linked via C−H···O interaction between the nitro oxygen O6 and O9 with the aromatic hydrogens H8 and H16, respectively, creating a three-dimensional hydrogen bonded network (Supporting Information).

3.1.3. Polymorph III. This form crystallizes in the orthorhombic space group *Pna*2(1) with $Z = 4$ and $R_{int} = 0.1149$. Although the unit cell is almost exactly metrically tetragonal, the molecule could not be solved as such in the tetragonal space group, probably because of the high R_{int} value of 0.4201. An ORTEP plot of polymorph III is shown in Figure 3a along with the atom numbering scheme. The conformation involving the torsional angle τ_{ether} ($N1_{amino}$−C−C−O_{ether}) is distinctly different from form II but similar to form I with respect to the torsional angle involving the arm composed of the ethereal oxygen O7. However, the difference could be observed for the other two arms composed of the ethereal oxygens O1 and O4 that are in the folded conformation, showing a change of 5.89° and 13.22°, respectively (Table 2). Structural analysis revealed that the tripodal moieties are stabilized by a considerably weak C−H···π interaction and intermolecular C−H···O hydrogen bonding interactions between the alkyl hydrogen from all three arms with one of the oxygens from each nitro group, unlike in forms II and III. It is interesting to note that the alkyl hydrogen H18B is involved in intermolecular C−H···π interaction with the electron deficient nitrophenyl ring belonging to the identical arm of neighboring tripodal units, resulting in a one-dimensional stacking of tripodal moieties along the *c*-axis. Each of these tripodal units are further involved in C−H···π interaction between the aromatic hydrogen H8 and the phenyl ring from a similar arm of adjacent tripodal units, generating a brick-wall kind of arrangement along the crystallographic *c*-axis (Figure 3b). However, it is not possible to conclude definitively if a C−C bond of the phenyl ring or the ring as a whole (centroid) is more significant with respect to C−H···π hydrogen bonding. Details of these interactions are as follows: for C8−H8···C1g, C8···C1g = 4.056 Å and ∠C8−H8···C1g = 151.63°, and for C18−H18B···C3g, C18···C3g = 4.058 Å and ∠C18−H18B···C3g = 151.44 Å. The nitro oxygens O3 and O5 are engaged in bifurcated acceptor hydrogen bonding to alkyl hydrogen H10A, H16 and H2A, H2B, respectively, whereas O8 is in interaction with the aromatic hydrogen H5, presenting a three-dimensional arrangement of C−H···O hydrogen bonds with C···O distances and C−H···O angles ranging from 3.221 to 3.399 Å and from 120.66 to 147.29°, respectively (Table 3). The crystal packing viewed along the *ab* plane shows that the tripodal units are alternately and antiparallelly arranged, with the apical nitrogen of each unit slightly tilted up and down in sequence along the *a* axis (Supporting Information).

Table 3. Relevant C−H···O Hydrogen Bond Interaction Data for Polymorphs I, II, and III

D−H···A	*d*(H···A) (Å)	*d*(D···A) (Å)	∠(DHA) (deg)
	Polymorph-I		
C24−H24···O3	2.674	3.557	158.63
C17−H17A···O5	2.566	3.520	167.72
C4−H4···O6	2.596	3.283	131.03
C8−H8···O8	2.431	3.156	134.86
C15−H15···O9	2.629	3.424	143.80
C23−H23···O9	2.570	3.135	119.51
	Polymorph-II		
C8−H8···O6	2.443	3.349	164.28
C9−H9A···O8	2.587	3.506	158.35
C16−H16···O9	2.684	3.549	155.24
	Polymorph-III		
C5−H5···O8	2.515	3.285	140.27
C2−H2A···O5	2.515	3.373	147.29
C2−H2B···O5	2.672	3.275	120.66
C10−H10A···O3	2.629	3.399	136.50
C16−H16···O3	2.631	3.221	121.87

3.2. Rationalization of Structural Features. Polymorphs I, II, and III crystallize in three different crystal systems: triclinic ($P\bar{1}$), monoclinic ($P2_1/n$), and orthorhombic (*Pna*2(1)), respectively. Polymorph I has two identical molecules in the unit cell, whereas polymorphs II and III have four molecules each. Crystal structure analyses of the polymorphs reveal the absence of any noncovalent interactions between the receptor arms, which might probably be responsible for the flat and extended orientations of the arms in polymorphs I and III, whereas there is an intramolecular edge-to-face interaction between the phenyl rings of the two proximal arms in form II. The molecules in different forms differ significantly in the torsional angle τ_{amino} (C−$N1_{amino}$−C−C), and notable changes are also observed in torsion τ_{ether} ($N1_{amino}$−C−C−O_{ether}) of form II compared to relatively small differences in forms I and III. Almost negligible changes are observed in torsion τ_{phenyl} (C−C−O_{ether}−C_{phenyl}) of the three polymorphs. Four of the six torsional angles τ_{amino} are in the folded conformation, and two are in the extended conformation in all three polymorphs, but significant differences could be well observed if we examine their torsional angle values. Upon examining the torsion angles in the polymorphic structures (Table 2), it appears that the polymorphism is indeed a result of the conformational flexibility of the single molecule. Significant differences are also observed in most covalent bond lengths and angles between the polymorphs, notably the amino C−N_{amino}−C angle is considerably greater in form II than in other polymorphs for all the three arms

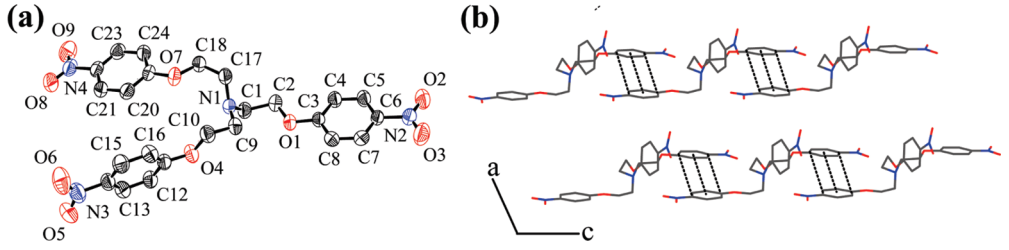

Figure 2. (a) ORTEP plot (50% probability ellipsoids) of polymorph II and (b) $\pi\cdots\pi$ stacking interaction in polymorph II along the *c* axis.

and small but notable changes are also reflected from the bond angle involving $N_{amino}-C-C$ of the three forms (Supporting Information). The nitro group from one of the arms of each polymorph is appreciably twisted out of the phenyl plane by 8.88°(3), 14.04°(2), and 12.54°(6), involving nitrogen N3 in polymorphs I and II and N4 in polymorph III, respectively, but it is approximately coplanar with the phenyl ring for the other two arms in the three polymorphs. Polymorph II exhibits an intermolecular nitro−nitro interaction which is not observed in the cases of polymorphs I and III. The crystal packing is significantly different in different polymorphs because of the different combination of noncovalent interactions in each polymorph. In polymorph I, all three nitro groups are involved in making six C−H···O hydrogen bonds through five oxygen atoms, whereas, in polymorph II, two nitro groups involving the nitrogen N3 and N4 are occupied in three hydrogen bonds via three oxygen atoms. In contrast to polymorphs I and II, five C−H···O hydrogen bonding interactions are exhibited by polymorph III involving one of the oxygen atoms from each nitro group. Polymorphs I and III are involved in one and two bifurcated C−H···O hydrogen bonds, respectively, while polymorph II exhibited no bifurcated hydrogen bond. Most importantly, the supramolecular features in the three forms are guided by the control of the methylene $C-H\cdots N_{amino}$ dimeric interaction in form I, $\pi\cdots\pi$ interactions in form II, and weak $C-H\cdots\pi$ interaction in form III that differentiate the overall packing in the three polymorphs (Supporting Information).

3.3. Crystal Growth and Habit. The morphology of the crystal is another important manifestation of the quality of the final products besides the crystal structure (Figure 4) Regular-shaped crystals are generally more favorable over anomalistic ones with respect to the practical usability. Different crystallization parameters such as the type of the solvent, the average levels of supersaturation, and so on are important to obtain a desired crystal habit. The polarity of the solvent is one of the most important properties that may affect the habit of the growing crystal. Different solvents will have different types of noncovalent interactions in the crystal lattice with the podand molecule, which will change the macroscopically crystal habit. Compound **L** is a polar molecule with a tertiary nitrogen atom and three active nitro groups, the presence of which facilitate the formation of several intermolecular noncovalent interactions among the tripodal units or possibly with solvent molecules, thus further affecting the habit of the crystals (Figure 4). The relationship between the crystal structure and morphology and external crystallization conditions is complex. Compound L was crystallized at room temperature from a library of solvents and binary solvent mixtures by slow evaporation of homogeneous and saturated solutions until single crystals were harvested with solvent remaining or almost evaporated. All crystallization experiments were conducted in an unmodified atmosphere. In the representative crystallization of polymorph I, 100 mg of compound was dissolved in 6 mL of acetonitrile or 0.5 mL of DMSO in a test tube at room temperature. The test tube was sealed with aluminum foil with a number of holes poked with a needle and allowed to stand undisturbed for several days, leading to the formation of thin yellow blocks of polymorph I, confirmed by examining the PXRD pattern of the crystallization batch and also comparison with the simulated pattern based on the single crystal structure determination. Slow evaporation of a saturated solution of **L** in a 3:1 binary solvent mixture of ethanol and acetic acid yielded high quality rhomboid shaped crystals of polymorph II within 2−3 weeks. Polymorph III was obtained from a saturated solution of 3:1 DMSO and acetic acid solvent mixture that has reproducibly afforded thin light yellow needles. It is worth mentioning that crystallization from ethanol yielded both blocky and rhomboid shape crystals of form I and II, respectively, with proportionally greater quantities of form II, which could be well separated with the help of a needle due to their different morphologies. The concomitant formation of polymorphs I and II from ethanol leads us to carry out the crystallization in a highly protic medium of an ethanol−acetic acid solvent mixture which yielded exclusively form II. Since form I has been obtained exclusively from aprotic solvents (acetonitrile/DMSO), concomitant crystallization of forms I and II from ethanol gave us an indication of whether crystallization in a

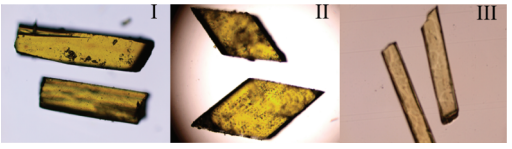

Figure 4. Optical micrograph images highlighting the different morphologies of three polymorphs of **L**.

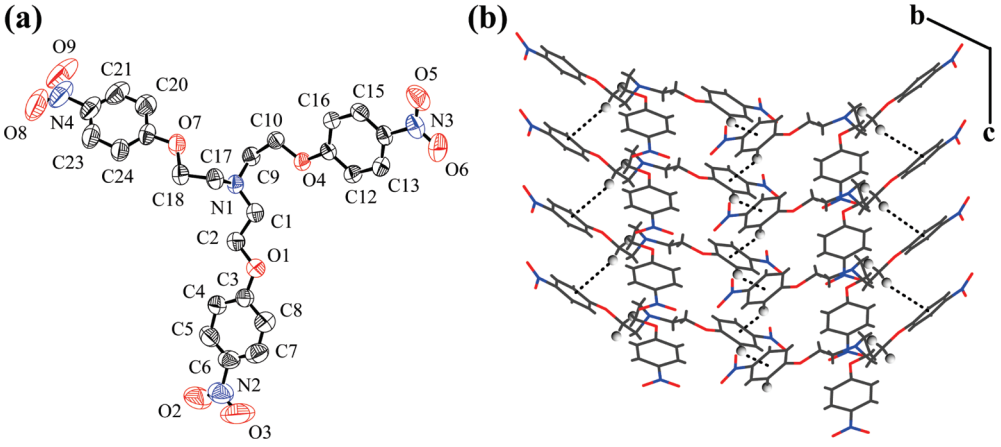

Figure 3. (a) ORTEP plot (50% probability ellipsoids) of polymorph III and (b) $C-H\cdots\pi$ stacking interaction in polymorph III along the *c* axis.

highly protic medium might help us in generating only a single polymorph of **L**. To investigate the influence of polar solvent and temperature in controlling polymorphic structure,[24] we have crystallized **L** by refluxing an ethanolic solution for 3−4 h, allowed it to cool at room temperature, and transferred it into a test tube for slow evaporation of the solvent, which exclusively yielded polymorph III. In spite of our repeated efforts, we were unable to obtain single crystals of **L** suitable for single crystal analysis from low boiling solvents such as DCM, chloroform, ethyl acetate, THF, and methanol, and we always ended up having powders which were found to contain a mixture of forms I and II (Supporting Information) when analyzed by PXRD. The crystallization experiments in different solvents showed that the polymorphic formation of **L** is essentially guided by the nature of the solvent.

3.4. Phase Behaviors of Polymorphs. Polymorphs I and II are quite stable at room temperature, but form III has been observed to undergo a solid to solid phase transition to form I at room temperature on storage over a period of about one month or so, which was confirmed by PXRD and DSC analyses. This simple observation argues strongly for the metastable nature of polymorph III. More quantitative evidence for the stability of polymorphs I and II and the metastability of form III was obtained by differential scanning calorimetry (DSC). DSC was conducted to investigate the thermal properties of the three polymorphs, shown in Figure 5. Measurements were carried out on all the forms in three cycles: (1) heating from room temperature (25 °C) to 150 °C; (2) cooling from 150 to 25 °C; and (3) reheating from 25 to 150 °C. In all cycles, heating and cooling rates of 2 °C/min were used. Each sample was prepared in two ways: crushed and uncrushed crystals between the two aluminum pans. No significant differences were observed in DSC traces. Form I shows only one endothermic peak at 109 °C corresponding to melting of the polymorph with an onset temperature of 104 °C, and no phase transition is detected. Form II displays a melting endotherm at 106.5 °C with the onset temperature near 98 °C; the DSC trace is otherwise featureless. Different from I and II, form III shows two endothermic peaks. The first peak at 105 °C with an onset temperature of 100 °C appears to be the solid-to-solid phase transition to the more stable polymorph I while the second endotherm with an onset of 106.0 °C and a peak at 108 °C coincides with the melting of form I (confirmed by PXRD). As all of the DSC samples were cooled to ambient temperature after heating, no thermal event was observed during the cooling, indicating super cooled liquids were likely formed. The melting endotherms of form I and II differ considerably by 2.5 °C and also show differences in the breadth of the melting ranges. Form II has a comparatively broader range of melting (∼15 °C) than form I (∼10 °C), also suggesting the fact that form II has a slightly lower melting point than form I (Figure 5). Thus, on completion of the DSC analysis, it can be concluded that transformation of polymorph III to the more stable polymorph I is kinetically very facile, as transformation can also be observed at room temperature and the transition is most likely to be monotropic. Furthermore, the enthalpies of transformation of the three forms calculated from the DSC data are found to be −398, −474, and −120 kJ mol^{-1} for polymorphs I, II, and III, respectively.

The PXRD is an important tool to determine the crystalline nature of the bulk sample. Figure 6 shows the PXRD patterns of each polymorphic form collected at room

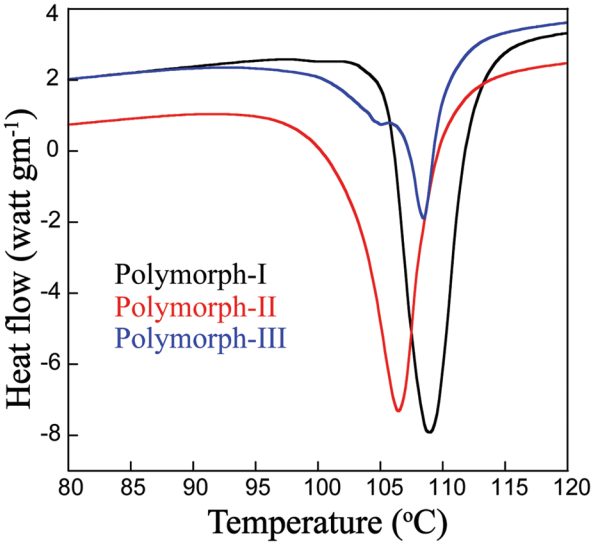

Figure 5. DSC thermographs of polymorphs I, II, and III.

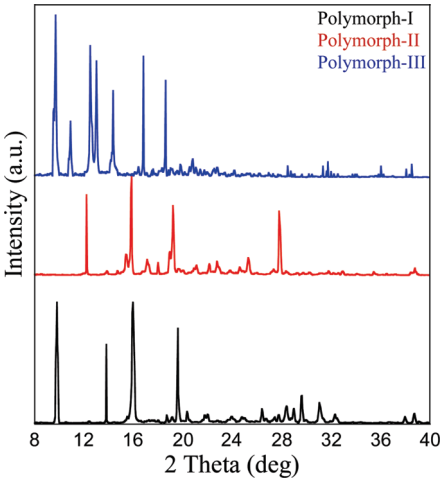

Figure 6. Experimental powder X-ray diffraction patterns of the three polymorphs.

temperature, which confirm clearly that they represent different crystalline phases. The comparison with the simulated patterns (Supporting Information) of all forms that are based on the single crystal structures determined at 298 K suggests that each crystallization batch was most likely of one single polymorph, not a mixture of multiple polymorphs. The differences in the position and intensity of the diffraction peaks indicate different possible crystal structures of **L** with preferable geometrical orientation. These differences in bulk crystalline properties are in agreement with the difference in their crystal structures. FT-IR spectra of each polymorph collected at room temperature also indicate different crystalline phases (Supporting Information). Though significant differences were not observed in the mid-IR region between the different polymorphic forms, notable changes could be observed in the far IR and fingerprint regions arising from the structural differences (*e.g.*, the different hydrogen-bonding arrangements).

4. Conclusion

In summary, we describe the conformational polymorphism of a nitro functionalized tripodal podand for the first

time. Compound **L** exhibits conformational polymorphism which results from the intrinsic conformational flexibility of the molecule around the tertiary amino group and yields an unprecedented set of three polymorphic forms by means of traditional solvent induced crystallization. Remarkable differences in the torsional angle values of τ_{amino} and τ_{ether} in all three polymorphs could possibly be the primary aspect for different orientations of the tripodal arms around the apical nitrogen. The crystals of different polymorphs exhibit different three-dimensional (3D) C−H···O hydrogen-bonding arrangements together with other noncovalent interactions. Considering the current intense interest in the phenomenon of polymorphism, together with its importance to the field of crystal chemistry, it is remarkable that all three of the polymorphs described here can apparently only be obtained as single crystals from the desired solvent used, and these preparations are reproducible. Thus, it may be concluded from the above studies that the prenucleation aggregates assemble in different supramolecular configurations depending on the use of solvent combinations. However, it is not easy to formulate a mechanism for polymorph induction based on solvent polarity due to the complexity of the molecule. Although a wide range of experimental conditions for producing polymorphs of **L** have been considered in the present work, it would not be surprising if further polymorphs of L are found in the future. Indeed, our attempts to search for polymorphs have been confined only to conventional crystallization procedures from solution. A wide range of other strategies provide the potential to generate further polymorphic forms, some of which are currently being explored in our ongoing research. A systematic survey of solvent-mediated polymorph generation in systems of this type, which involves crystal structure studies of several substituted tripodal molecules in terms of careful modeling studies and charge density analyses, is currently being pursued to get further insights into the nature of their packing modes. Therefore, due to the interesting structural and phase properties, the crystal system may provide an excellent case for understanding crystal growth and crystal packing.

Acknowledgment. G.D. acknowledges DST (SR/S1/IC-01/2008) and CSIR (01-2235/08/EMR-II), New Delhi, India, for financial support; DST-FIST for its single crystal X-ray diffraction facility; and Centre for Nanotechnology for powder X-ray diffraction and CIF, IIT Guwahati.

Supporting Information Available: Crystal structures of the three polymorphs in the form of crystallographic information files (CIF), bond parameters, angle parameters, and crystal packing diagrams. This material is available free of charge via the Internet at http://pubs.acs.org.

References

(1) McCrone, W. C. In *Physics and Chemistry of the Organic Solid State*; Fox, D., Labes, M. M., Weissberger, A., Eds.; Interscience Publishers: New York, 1965; Vol. 2, pp 725−767.

(2) Long, S.; Parkin, S.; Siegler, M. A.; Cammers, A.; Li, T. *Cryst. Growth Des.* **2008**, *8*, 4006. (b) Chandran, S. K.; Nath, N. K.; Roy, S.; Nangia, A. *Cryst. Growth Des.* **2008**, *8*, 140.

(3) (a) Polymorphism and Crystallization. *Org. Process Res. Dev.* **2000**, *4*, 371.(b) Polymorphism in Crystals: Fundamentals, Prediction and Industrial Practice. *Cryst. Growth Des.* **2003**, *3*, 867. International Conferences: (c) Polymorphism in Crystals: Fundamentals, Prediction and Industrial Practice, Saddlebrook Resort, Tampa, FL, Feb 2003. (d) Diversity Amidst Similarity: a Multidisciplinary Approach to Polymorphs, Solvates and Phase Relationships, 35th Course: International School of Crystallography, June 9−20, Erice, Sicily, Italy, **2004**. (e) Sarma, J. A. R. P.; Desiraju, G. R. In *Crystal Engineering: Polymorphism and Pseudopolymorphism in Organic Crystals: A Cambridge Structural Database Study*; Seddon, S. R., Zaworotko, M., Eds.; Kluwer: Norwell, MA, 1999; p 325. (f) Desiraju, G. R. *Science* **1996**, *278*, 404.

(4) Long, S.; Parkin, S.; Siegler, M. A.; Cammers, A.; Li, T. *Cryst. Growth Des.* **2008**, *8*, 4006–4013.

(5) (a) Threlfall, T. *Org. Process Res. Dev.* **2000**, *4*, 384. (b) Jetti, R. K. R.; Boese, R.; Sarma, J. A. R. P.; Reddy, L. S.; Vishweshwar, P.; Desiraju, G. R. *Angew. Chem., Int. Ed.* **2003**, *42*, 1963. (c) Davey, R. J.; Blagden, N.; Righini, S.; Alison, S.; Quayle, M. J.; Fuller, S. *Cryst. Growth Des.* **2001**, *1*, 59.

(6) (a) Bernstein, J. *Polymorphism in Molecular Crystals*; Oxford University Press: Oxford, 2002. (b) Threlfall, T. L. *Analyst* **1995**, *120*, 2435. (c) Davey, R. J. *Chem. Commun.* **2003**, 1463. (d) Byrn, S. R.; Pfeiffer, R. R.; Stowell, J. G. *Solid-State Chemistry of Drugs*; SSCI: West Lafayette, IN, 1999.

(7) (a) Nangia, A. *Acc. Chem. Res.* **2008**, *41*, 595. (b) Desiraju, G. R. *Acc. Chem. Res.* **1996**, *29*, 441. (c) Desiraju, G. R. *Acc. Chem. Res.* **2002**, *35*, 565.

(8) Desiraju, G. R. *Angew. Chem., Int. Ed. Engl.* **1995**, *34*, 2311.

(9) (a) Bilton, C.; Howard, J. A. K.; Madhavi, N. N. L.; Nangia, A.; Desiraju, G. R.; Allen, F. H.; Wilson, C. C. *Chem. Commun.* **1999**, 1675. (b) Kumar, V. S. S.; Addlagatta, A.; Nangia, A.; Robinson, W. T.; Broder, C. K.; Mondal, R.; Evans, I. R.; Howard, J. A. K.; Allen, F. H. *Angew. Chem., Int. Ed.* **2002**, *41*, 3848. (c) Chen, S.; Guzei, I. A.; Yu, L. *J. Am. Chem. Soc.* **2005**, *127*, 9881.

(10) (a) *Polymorphism in Pharmaceutical Solids*; Brittain, H. G., Ed.; Marcel Dekker: New York, 1999. (b) Byrn, S. R.; Pfeiffer, R. R.; Stowell, J. G. *Solid State Chemistry of Drugs*, 2nd ed.; SSCI, Inc.: West Lafayette, IN, 1999. (c) Vishweshwar, P.; McMahon, J. A.; Oliveira, M.; Peterson, M. L.; Zaworotko, M. J. *J. Am. Chem. Soc.* **2005**, *127*, 16802. (d) Fabbiania, F. P. A.; Allan, D. R.; Parsons, S.; Pulham, C. R. *CrystEngComm* **2005**, *7*, 179. (e) Prusiner, P.; Sundaralingam, M. *Acta Crystallogr.* **1976**, *B32*, 419. (f) Brittain, H. G. *J. Pharm. Sci.* **2007**, *96*, 705. (g) Vippagunta, S. R.; Brittain, H. G.; Grant, D. J. W. *Adv. Drug Delivery Rev.* **2001**, *48*, 3.

(11) (a) Bernstein, J. In *Organic Solid State Chemistry*; Desiraju, G. R., Eds.; Elsevier: Amsterdam, 1987; Vol. 32, pp 471−518. (b) Gavezzotti, A.; Fillippini, G. *J. Am. Chem. Soc.* **1995**, *117*, 12299. (c) Jacques, J.; Collet, A.; Wilen, S. H. *Enantiomers, Racemates, and Resolutions*; Krieger Publishing Company: Malabar, FL, 1991. (d) Brock, C. P.; Schweizer, W. B.; Dunitz, J. D. *J. Am. Chem. Soc.* **1991**, *113*, 9811.

(12) (a) Buttar, D.; Charlton, M. H.; Docherty, R.; Starbuck, J. *J. Chem. Soc., Perkin Trans.* **1998**, *2*, 763–772. (b) Starbuck, J.; Docherty, R.; Charlton, M. H.; Buttar, D. *J. Chem. Soc., Perkin Trans.* **1999**, *2*, 677–691.

(13) (a) Staab, E.; Addadi, L.; Leiserowitz, L.; Lahav, M. *Adv. Mater.* **1990**, *2*, 40. (b) Davey, R. J.; Blagden, N.; Potts, G. D.; Docherty, R. *J. Am. Chem. Soc.* **1997**, *119*, 1767–1772. (c) Bonafede, S.; Ward, M. *J. Am. Chem. Soc.* **1995**, *117*, 7853–7861. (d) Bernstein, J.; Davey, R. J.; Henck, J.-O. *Angew. Chem., Int. Ed.* **1999**, *38*, 3441–3461.

(14) Gavezzotti, A. *Acc. Chem. Res.* **1994**, *27*, 7153–7157.

(15) Desiraju, G. R. *Crystal Engineering The Design of Organic Solids*; Elsevier: New York 1989.

(16) (a) Martínez-Manez, R.; Sancenon, F. *Chem. Rev.* **2003**, *103*, 4419. (b) Wu, B.; Liang, J.; Yang, J.; Jia, C.; Yang, X.; Zhang, H.; Tangb, N.; Janiakc, C. *Chem. Commun.* **2008**, 1762. (c) Lakshminarayanan, P. S.; Ravikumar, I.; Suresh, E.; Ghosh, P. *Chem. Commun.* **2007**, 5214. (d) Lakshminarayanan, P. S.; Suresh, E.; Ghosh, P. *Inorg. Chem.* **2006**, *45*, 4372.

(17) Shum, S. P.; Pastor, S. D.; DeBellis, A. D.; Odorisio, P. A.; Burke, L.; Clarke, F. H.; Rihs, G.; Piatek, B.; Rodebaugh, R. K. *Inorg. Chem.* **2003**, *42*, 5097.

(18) (a) Pramanik, A.; Das, G. *Tetrahedron* **2009**, *65*, 2196. (b) Pramanik, A.; Bhuyan, M.; Das, G. *J. Photochem. Photobiol. A* **2008**, *197*, 149. (c) Pramanik, A.; Bhuyan, M.; Choudhury, R.; Das, G. *J. Mol. Struct.* **2008**, *879*, 88.

(19) Singh, A. S.; Bharadwaj, P. K. *Dalton Trans.* **2008**, 738.

(20) *SMART, SAINT and XPREP*; Siemens Analytical X-ray Instruments Inc.: Madison, WI, 1995.

(21) Sheldrick, G. M. *SADABS: software for Empirical Absorption Correction*; University of Gottingen, Institute fur Anorganische Chemieder Universitat: Tammanstrasse 4, D-3400, Gottingen, Germany, 1999−2003.

(22) Sheldrick, G. M. *SHELXS-97*; University of Gottingen: Germany, 1997.

(23) Farrugia, L. J. *J. Appl. Crystallogr.* **1997**, *30*, 565.

(24) Muthu, S.; Vittal, J. J. *Cryst. Growth Des.* **2004**, *4*, 1181–1184.